Optical Properties of Aggregated Metal Systems. I. Theory*

J. P. Marton
Welwyn Canada Limited, London, Ontario, Canada
and Institute for Materials Research, McMaster University, Hamilton, Ontario, Canada

and

J. R. Lemon
Welwyn Canada Limited, London, Ontario, Canada

(Received 17 February 1971)

In this part, the simplest optical theory of aggregated metal systems, due to Maxwell-Garnett, is analyzed. The complex dielectric constant of the system, and that of the constituent metal aggregates, are represented as transformations. The functions show single and double poles in certain regions of physical interest, indicating resonance behavior. These features are explored for free-electron metals, and an optical "conduction resonance" for the aggregated system is discovered. The resonance frequency and the magnitude of the optical conductivity are calculated, along with the plasma frequency and the magnitude of the bulk electron loss function. A relation between conduction and plasma resonances is established and it is found to be independent of the free-electron parameters of the metal. This, and other results, indicate that the conduction resonance is a macroscopic effect, being due to a collective polarization interaction between the constituent metal aggregates, and it may be looked upon as a kind of transverse plasma resonance. In the second part, the present results will be applied to real metals.

I. INTRODUCTION

Optical phenomena associated with aggregated metal systems have been the subject of many studies.[1-6] The scattering of light by submicroscopic metal aggregates, suspended in a dielectric medium, already attracted attention before the turn of the century.[1] Colloidal color centers in alkali halide crystals,[2] "anomalous" optical properties of thin metal films[3] and of surfaces of bulk metals,[4,5] and scattering by metal sols are areas of important current research. The material system, generally being composed of a dielectric matrix in which the metal aggregates are dispersed, may be specified phenomenologically by its complex frequency-dependent dielectric constant $\tilde{\mathcal{E}}(\omega) = \mathcal{E}_1(\omega) + i\mathcal{E}_2(\omega)$. Physically, the description of the system is given by the properties of the constituent metal and the dielectric. Theoretically, the optical properties of aggregated metal systems may be described in terms of the index of refraction of the dielectric matrix n, the frequency-dependent complex dielectric constant of the metal aggregates $\tilde{\epsilon}(\omega) = \epsilon_1(\omega) + i\epsilon_2(\omega)$, and the volume fraction of the metal q by the Maxwell-Garnett (MG) theory[6] as

$$[\tilde{\mathcal{E}}(\omega) - n^2]/[\tilde{\mathcal{E}}(\omega) + 2n^2] = q\,[\tilde{\epsilon}(\omega) - n^2]/[\tilde{\epsilon}(\omega) + 2n^2]\,. \tag{1}$$

In the theory, it is assumed that the metal aggregates are spherical, that they are much smaller than the wavelength of the incident light, and that they are randomly distributed in the dielectric matrix. The theory takes no precise account of the interaction between aggregates; rather, it considers the average affect of polarization on the interacting aggregates using the Lorentz correction to the local field. The size of the individual metal spheres is also irrelevant in the theory as long as it is much less than the wavelength of the incident light. Therefore the variation of size of aggregates is allowed. These approximations would appear to restrict the usefulness of the theory to systems where the aggregates are very small and are far apart, i.e., to systems with very small metal content. However, experimental evidence appears to suggest that the simple MG theory gives a good qualitative description of the optical properties of aggregated systems for all values of q, where $0 < q < 1$, but not for $q = 0$ and $q \approx 1$. Sennett and Scott[7] used the theory for aggregated metal films followed by other workers with good results. Recently, the theory was applied[5] to bulk metals with rough surfaces in an attempt to explain the Mayer anomaly[8] for alkali metals.

Improvements, aimed at overcoming some of the shortcomings of the MG theory, have been advanced. The aggregate size as a variable was introduced by Mie,[9] spherical geometry was replaced with rotational ellipsoids by Schopper,[10] and variation of the size of aggregates was taken into consideration by Yoshida *et al.*[11] These modifications improved the theoretical situation, but only at the expense of adding one or more new variables to the problem that was already six dimensional. Therefore, to avoid undue complications in the present work we shall use the simple MG theory.

With the exception of one recent effort, [12] the MG theory has not been analyzed algebraically in any detail, likely because of the multitude of variables involved and the consequent difficulty in visualizing the functional relations in terms of these variables. Some special features of the theory for thin metal films have been discussed by Marton[13] where the treatment was restricted to long wavelengths and free-electron-type metal aggregates. In the present work we give a general algebraic analysis of the theory, independent of any specific electronic model of the constituent metal aggregates. The results are then applied to free-electron metals, with special attention being paid to a sharp resonance in the optical conductivity and to the plasma resonance of the system. The consequences of the features are discussed and the optical behavior of an idealized system is analyzed as a typical example.

II. THEORY

In order to analyze Eq. (1), we make a complex-coordinate transformation, i.e., we map the complex function $\tilde{\mathcal{E}} = \mathcal{E}_1 + i\mathcal{E}_2$ on the complex field $\tilde{\epsilon} = \epsilon_1 + i\epsilon_2$, through the scalar quantity q. To carry out the transformation in the simplest manner, we assume the index of refraction for the dielectric matrix to be unity. The justification for this will become apparent later. We start then with the relation

$$(\tilde{\mathcal{E}} - 1)/(\tilde{\mathcal{E}} + 2) = q\,(\tilde{\epsilon} - 1)/(\tilde{\epsilon} + 2)\,, \tag{2}$$

where $\tilde{\mathcal{E}}$ is the complex dielectric constant of the system, and where the system is composed of q volume fraction of metal with complex dielectric constant $\tilde{\epsilon}$. For simplicity we dropped ω.

The object is to find the contours $\mathcal{E}_1 = \text{const}$ and $\mathcal{E}_2 = \text{const}$ in the Cartesian-coordinate system (ϵ_1, ϵ_2) for every value of q. Equating the real and imaginary parts in (2) we get

$$\mathcal{E}_1 = \frac{(\epsilon_1^2 + \epsilon_2^2)(1+2q)(1-q) + \epsilon_1(4q^2+q+4) + 2(1-q)(q+2)}{(\epsilon_1^2 + \epsilon_2^2)(1-q)^2 + 2\epsilon_1(1-q)(q+2) + (q+2)^2} \tag{3}$$

and

$$\mathcal{E}_2 = \frac{9q\,\epsilon_2}{(\epsilon_1^2 + \epsilon_2^2)(1-q)^2 + 2\epsilon_1(1-q)(q+2) + (q+2)^2}\,. \tag{4}$$

Now set $\mathcal{E}_1 = C_1$ in (3), and after some manipulation we get

$$\left(\epsilon_1 + \frac{(1-q)^2 + 0.5\,(1+2q)(2+q) - C_1(1-q)(2+q)}{(1+2q)(1-q) - C_1(1-q)^2}\right)^2 + \epsilon_2^2 = \left(\frac{4.5q}{(1+2q)(1-q) - C_1(1-q)^2}\right)^2\,. \tag{5}$$

This is recognized to be an equation of circles, i.e., $(\epsilon_1 + a)^2 + \epsilon_2^2 = r^2$, with centers on the ϵ_1 axis at position a and with radius r. We note from (5) that

$$a = r - (2+q)/(1-q)\,, \tag{6}$$

and since the second term on the right-hand side depends on q only, all circles C_1 for a given value of q must be passing through the point $-(2+q)/(1-q)$ on the ϵ_1 axis and be tangent to each other at that point. We also note from (5) that for a given value of q the radius r can have both positive and negative values. A positive radius means that the center of the circle is to the right of the point $-(2+q)/(1-q)$ on the ϵ_1 axis while a negative radius means the center is to the left. The radius may also be infinitely large. This is represented by a straight line, passing through the ϵ_1 axis at right angle, at $-(2+q)/(1-q)$. The $\mathcal{E}_1 = C_1$ contours are illustrated in Fig. 1(a) for $q = 0.7$, and for several values of C_1 in the (ϵ_1, ϵ_2) plane. The special position $-(2+q)/(1-q)$ on the ϵ_1 axis is apparent.

Now we find the $\mathcal{E}_2$ contours by setting $\mathcal{E}_2 = C_2$ in (4) and by putting the equation in the form

$$\left(\epsilon_1 + \frac{2+q}{1-q}\right)^2 + \left(\epsilon_2 - \frac{9q}{2C_2(1-q)^2}\right)^2 = \left(\frac{9q}{2C_2(1-q)^2}\right)^2\,. \tag{7}$$

This is also recognized to be an equation of circles, i.e., $(\epsilon_1 + b)^2 + (\epsilon_2 - d)^2 = R^2$. From Eqs. (6) and (7) we see that $b = r - a$, and $d = R$. This means that the centers of circles for a given value of q all lie on the line $\epsilon_1 = -(2+q)/(1-q)$, and that the circles are tangent to each other and to the ϵ_1 axis at this point on the ϵ_1 axis. The $\mathcal{E}_2 = C_2$ contours are illustrated in Fig. 1(b) for $q = 0.7$ and for several values of C_2 in the (ϵ_1, ϵ_2) plane. Note that the special position $-(2+q)/(1-q)$ on the ϵ_1 axis is the same as that for the $\mathcal{E}_1$ contours in Fig. 1(a).

Taken together, the $\mathcal{E}_1$ and $\mathcal{E}_2$ contours on the (ϵ_1, ϵ_2) plane for a given value of q represent the complete transformation for that value of q. The new coordinate system $(\mathcal{E}_1, \mathcal{E}_2)$ is orthogonal, and resembles the Smith chart, familiar to radio engineers. The coordinate systems $(\mathcal{E}_1, \mathcal{E}_2)$ mapped on

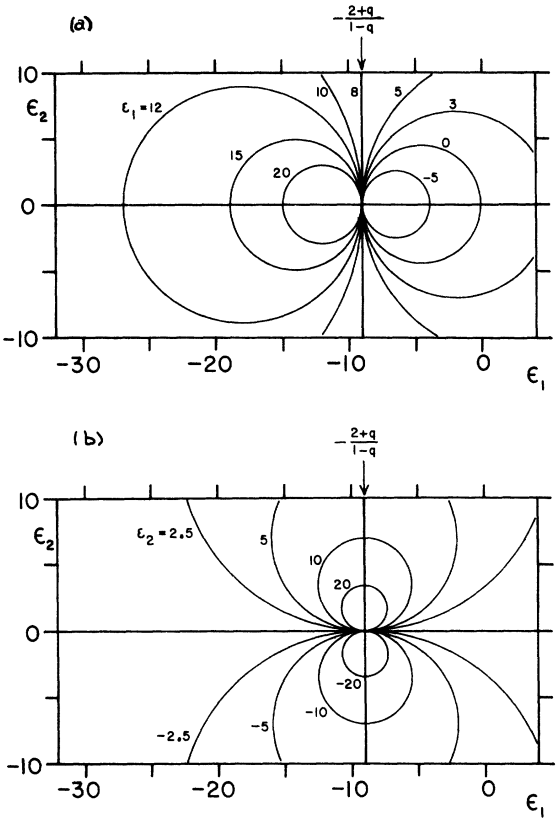

FIG. 1. (a) Contours of $\mathcal{S}_1 = C_1$ on the (ϵ_1, ϵ_2) plane for $q = 0.7$ as calculated from Eq. (5). Note the pole at $-(2+q)/(1-q)$ on the ϵ_1 axis. (b) Contours of $\mathcal{S}_2 = C_2$ on the (ϵ_1, ϵ_2) plane for $q = 0.7$ as calculated from Eq. (7). Note that the poles for $\mathcal{S}_2$ and $\mathcal{S}_1$ coincide.

the Cartesian plane (ϵ_1, ϵ_2) for several values of q are plotted in Fig. 2. The values of ϵ_2 were restricted to the physically meaningful domain of $\epsilon_2 \geq 0$. This figure shows the general features of Eq. (2) in all of its five variables. It becomes clear now why we had to take $n = 1$ in Eq. (1). Had we chosen n to remain as a variable, it would have added another dimension to the problem and prevented us from visualizing the transformation graphically. Moreover, values of n different from unity do not affect the general features of the maps in Fig. 2, they merely shift the values of some of the coordinates.

It is apparent from Fig. 2 that for all q values the point $[\epsilon_1 = -(2+q)/(1-q),\ \epsilon_2 = 0]$ is a pole for both functions $\mathcal{S}_1$ and $\mathcal{S}_2$. The pole of $\mathcal{S}_2$ is positive, while $\mathcal{S}_1$ has a negative pole at the right, and a positive pole at the left of this point. For small q values the poles are at $[\epsilon_1 = -2,\ \epsilon_2 = 0]$, and for large q values they shift to large negative ϵ_1 values. At $q = 1$, we get $[\epsilon_1 = -\infty,\ \epsilon_2 = 0]$ for the poles. Also, for this value of q the $\mathcal{S}$ contours become straight lines and we have $(\mathcal{S}_1, \mathcal{S}_2) = (\epsilon_1, \epsilon_2)$ as expected from Eqs. (3) and (4). On physical grounds, we exclude from the present consideration values

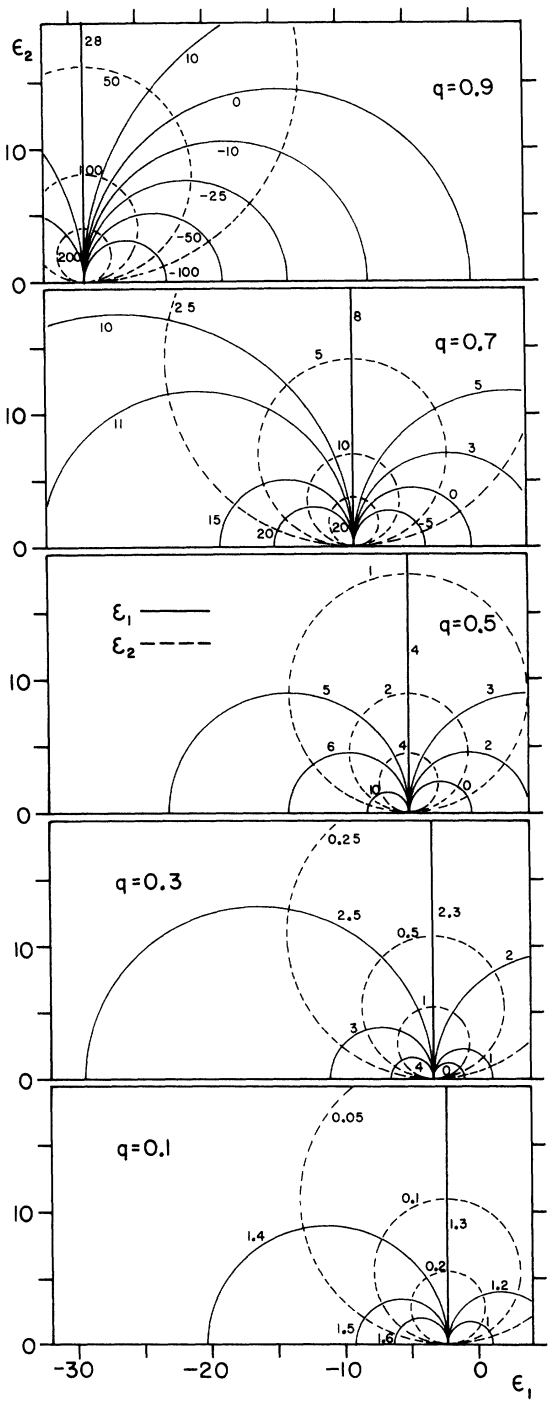

FIG. 2. Coordinate system $(\mathcal{S}_1, \mathcal{S}_2)$ mapped on the Cartesian plane (ϵ_1, ϵ_2) for several values of q, representing the complete MG transformation according to Eqs. (5) and (7). Transformation is restricted to the physically meaningful region of $\epsilon_2 \geq 0$.

of q equal to zero or unity and those that are close to one, since for $q=0$ or $q=1$ we get, respectively, the trivial cases of a purely dielectric or a purely metallic medium, while for $q \approx 1$ the assumptions of the MG theory do not hold. However, we do allow values of q up to 0.9 for completeness,[14] but will take the necessary precautions in the interpretations of the results.

III. FREE-ELECTRON METALS

Consider a system of metal aggregates in a dielectric medium, where the system satisfies the assumptions of the MG theory, and where the index of refraction of the dielectric is unity. Let the metal aggregates be the free-electron type, characterized by the plasma frequency $\omega_p = (4\pi Ne^2/m^*)^{1/2}$ and the relaxation time τ of the free electrons. Here e, N, and m^* are, respectively, the charge, the number density, and the effective mass of the conduction electrons. Let us examine the optical properties of the system at frequency ω. The real and imaginary parts of the frequency-dependent complex dielectric constants of the free-electron metal aggregates are given, respectively, by the simple Drude theory as

$$\epsilon_1 = 1 - (\omega_p^2 \tau^2)/(1+\omega^2\tau^2) \tag{8}$$

and

$$\epsilon_2 = (\omega_p^2 \tau^2)/[\omega(1+\omega^2\tau^2)]\,. \tag{9}$$

To obtain the complete frequency and q dependencies of the dielectric constants $\mathcal{E}_1$ and $\mathcal{E}_2$ of a system for a given metal, having given values of ω_p and τ, we should substitute functions (8) and (9) into (3) and (4). This approach would lead to unmanageable algebra and give no useful solution. Instead, we approach the problem graphically, by plotting functions (8) and (9) on the complex MG maps developed above. The solution for $\mathcal{E}_1(\omega, q)$ and $\mathcal{E}_2(\omega, q)$ for a given metal is readily provided by the maps, by simply reading the intersections of the plot and the $\mathcal{E}_1$ and $\mathcal{E}_2$ axes. An example[15] of the approach is given in Fig. 3, for $q=0.7$, $\hbar\omega_p = 6.6$ eV and $\tau = 2.6\times10^{-14}$ sec. The dielectric constants of the metal itself, $\epsilon_1(\omega)$ and $\epsilon_2(\omega)$, as well as those of the system, $\mathcal{E}_1(\omega, q)$ and $\mathcal{E}_2(\omega, q)$, with the same parameters q, ω_p, and τ are replotted in a more conventional fashion in Figs. 4(a) and 4(b). The difference between the dielectric constants $\tilde{\epsilon}$ and $\tilde{\mathcal{E}}$ are apparent from the figures. The main feature of the transformed quantities $\tilde{\mathcal{E}}$ is a resonance in $\mathcal{E}_2$ at a frequency where $\mathcal{E}_1 \approx 0$. This is reminiscent of another resonance, at the frequency where the real part ϵ_1 of the dielectric constant for free-electron metals is zero, i.e., the bulk plasma resonance.

Plasma resonance is indicated by a peak in the bulk electron energy-loss function (L_B), defined in terms of the dielectric constants as

$$L_B = -\operatorname{Im}\tilde{\epsilon}^{-1}\,. \tag{10}$$

Applying the same definition to the transformed dielectric constants $\tilde{\mathcal{E}}$, we expect a peak in the loss function $-\operatorname{Im}\tilde{\mathcal{E}}^{-1}$ at the frequency or frequencies where $\mathcal{E}_1 \approx 0$. In Fig. 4(c) we plot L_B for both $\tilde{\epsilon}$ and $\tilde{\mathcal{E}}$ and see that in both cases there is only one peak. Further, we see that the resonance in L_B for $\tilde{\mathcal{E}}$ does not coincide with the resonance in $\mathcal{E}_2$ in Fig. 4(b). Rather, the two resonances correspond to the two frequencies at which $\mathcal{E}_1 = 0$ in Fig. 4(a). For the free-electron system, there is only one resonance frequency at $\epsilon_1 \approx 0$ and that corresponds to the bulk plasma resonance.

From the foregoing we may conclude that the resonance in $\mathcal{E}_2$ is not due to plasma in the usual sense. We denote the frequency at $\mathcal{E}_2$ resonance ω_R', and call the feature "optical conduction reso-

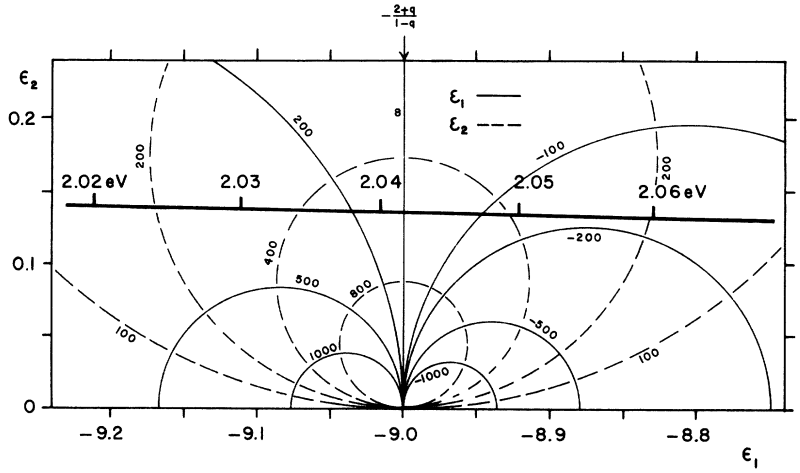

FIG. 3. Free-electron curve plotted on the map for $q=0.7$. The free-electron parameters ω_p and τ were given values for this figure as well as all subsequent ones of $\hbar\omega_p = 6.6$ eV and $\tau = 2.6\times10^{-14}$ sec being typical of good conductors. Frequency dependence is indicated by the photon energy in eV marked opposite the curve. Note that all the relevant variables, i.e., ϵ_1, ϵ_2, $\mathcal{E}_1$, $\mathcal{E}_2$, q, ω_p, τ, and ω, are contained in the figure.

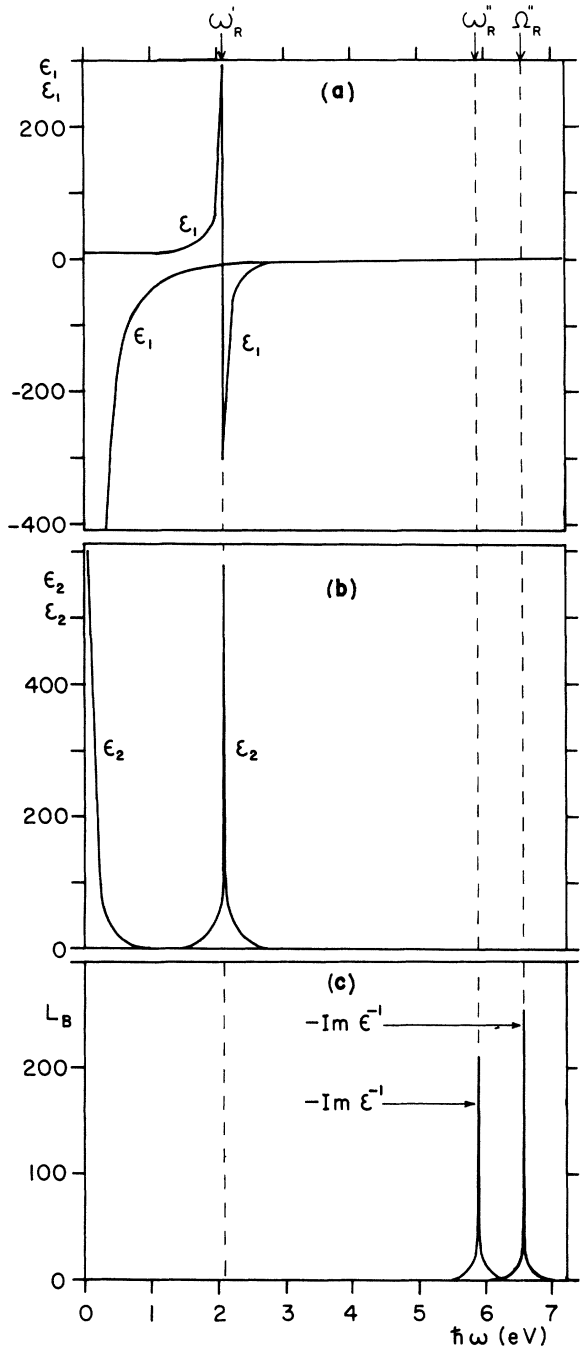

FIG. 4. Free-electron quantities used in Fig. 3 for $q = 0.7$ are replotted as functions of ω in a more conventional fashion. (a) Real parts of dielectric constants ϵ_1 (free electron) and $\mathcal{E}_1$ (aggregate system); (b) imaginary parts of dielectric constants ϵ_2 (free electron) and $\mathcal{E}_2$ (aggregated system); and (c) the bulk electron energy-loss functions of the free-electron metal and the aggregated system. Note the frequencies ω_R', ω_R'', and Ω_R'' at which resonances occur.

nance." The reason for the name will be apparent later. The plasma resonance frequency for $\bar{\mathcal{E}}$ is denoted by ω_R'', and that for ϵ by Ω_R''. In the example, we find $\omega_R' < \omega_R''$ and $\omega_R'' < \Omega_R''$.

For free-electron metals, we know that the resonance frequency of the damped plasma Ω_R'' is related to the plasma frequency ω_p by

$$\Omega_R'' = (\omega_p^2 - 1/\tau^2)^{1/2} , \tag{11}$$

and now we seek expressions for the resonance frequencies ω_R' and ω_R'' of the aggregated system. We proceed by calculating ω_R' and ω_R'' from Eqs. (3), (4), (8), and (9), assuming that both conduction and plasma resonances occur at frequencies for which $\mathcal{E}_1 = 0$. Thus we set the numerator of (3) equal to zero and substitute ϵ_1 and ϵ_2 from (8) and (9). This gives

$$9B^6 + [18 - 3(2+q)A^2] \times B^4 + [9 - 3(2+q)A^2 + (1+2q)(1+q)A^4] \times B^2 + (1+2q)(1-q)A^4 = 0 ,$$

where $A = \omega_p \tau$ and $B = \omega \tau$. The equation is cubic in the variable B^2 and an inspection shows that $B^2 = -1$ is a root. This root is of no physical interest so $B^2 + 1$ can be factored out, resulting in

$$9B^4 + [9 - 3(2+q)A^2]B^2 + (1+2q)(1-q)A^4 = 0 .$$

The equation is quadratic and the solution is

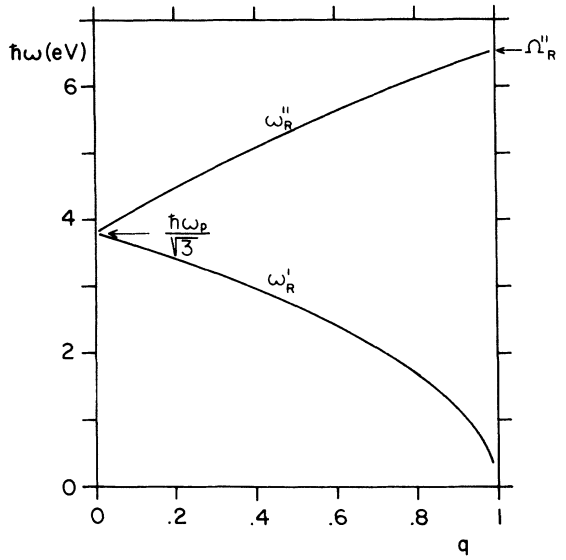

FIG. 5. Variation of resonance frequencies ω_R' and ω_R'' of the aggregated system with q for the example. Upper curve represents plasma resonance and the lower one gives the q dependence of the conduction resonance frequency. At small q values $\omega_R'' \approx \omega_R'$.

$$B^2 = \tfrac{1}{6}\{-3 + (2+q)A^2 \pm [9 - 6(2+q)A^2 + 9q^2A^4]^{1/2}\} . \tag{12}$$

It is easy to show that for B^2 to be real and positive the condition

$$A^2 \geq \{2 + q + 2[(1+2q)(1-q)]^{1/2}\}/3q^2$$

has to be satisfied. The two roots ω_R' and ω_R'' are thus

$$\begin{Bmatrix}\omega_R' \\ \omega_R''\end{Bmatrix} = \left(\frac{\omega_p^2\tau^2(2+q) - 3 \mp [9 - 6\omega_p^2\tau^2(2+q) + 9q^2\omega_p^4\tau^4]^{1/2}}{6\tau^2}\right)^{1/2} , \tag{13}$$

where the minus sign gives ω_R' and the plus sign gives ω_R''. The two resonance frequencies as functions of q for the example are plotted in Fig. 5. The upper curve represents the variation of plasma resonance frequency ω_R'' with q, and the lower curve gives the q dependence of the conduction resonance frequency ω_R'. At the lower limit of q, we have for ω_R' and ω_R''

$$q \to 0 , \quad \begin{Bmatrix}\omega_R' \\ \omega_R''\end{Bmatrix} \to \left(\tfrac{1}{3}\omega_p^2 - \frac{1}{\tau^2}\right)^{1/2} , \tag{14}$$

while at the upper limit of q, we get

$$\begin{aligned} &q \to 1, \quad \omega_R' \to 0 , \\ &q \to 1, \quad \omega_R'' \to (\omega_p^2 - 1/\tau^2)^{1/2} = \Omega_R'' . \end{aligned} \tag{15}$$

These limits are apparent from Fig. 5.

It remains to be shown that the conduction and plasma resonances for a free-electron metal aggregate system occur at the exact frequencies for which $\mathcal{E}_1 = 0$, i.e., that the assumption which led to (13) is correct. We prove this by showing that the appropriate functions have maxima at the resonance frequencies. For the conduction resonance, we take $\partial\mathcal{E}_2/\partial\omega$ from (4), substitute ϵ_1 and ϵ_2 from (8) and (9), and substitute the resonance frequency ω_R' from Eq. (13). After the necessary manipulations we find

$$\left(\frac{\partial\mathcal{E}_2}{\partial\omega}\right)_{\omega=\omega_R'} = 0 .$$

Similarly, we take $\partial(-\operatorname{Im}\tilde{\mathcal{E}}^{-1})/\partial\omega$ for the plasma resonance, substitute ϵ_1 and ϵ_2 from (8) and (9), substitute the resonance frequency ω_R'' from (13), carry out the necessary (and very large number of) steps in the algebra, and find

$$\left(\frac{\partial(-\operatorname{Im}\tilde{\mathcal{E}}^{-1})}{\partial\omega}\right)_{\omega=\omega_R''} = 0.$$

In the proof, we assumed that the resonances are not critically damped, i.e., that $\omega_p\tau > 1$, thus (13) is an exact relation only for free-electron systems satisfying this condition.

IV. CONDUCTION RESONANCE

In the derivation above we labeled the resonance feature in the $\mathcal{E}_2(\omega)$ curve at ω_R' optical conduction resonance. The reason for the particular choice is that we wish to consider the real part of the optical conductivity $\sigma(\omega)$, rather than the imaginary part of the optical dielectric constant $\mathcal{E}_2(\omega)$ in connection with the resonance.

To make the change, we introduce the conductivity for the aggregated system as $S(\omega) = \mathcal{E}_2\omega/4\pi$ and that for the free-electron metal as $\sigma(\omega) = \epsilon_2\omega/4\pi$. From (9), we see that $\sigma(\omega) = \sigma_0/(1+\omega^2\tau^2)$, where σ_0 is the dc conductivity given by $\sigma_0 = \omega_p^2\tau/4\pi$. The advantage of using the conductivity instead of the dielectric constant is that with $\omega \to 0$ we get $\sigma \to \sigma_0$, whereas at the same limit we have $\mathcal{E}_2 \to \infty$, which is undesirable. Now we wish to determine the magnitude of conductivity $S(\omega)$ at resonance ω_R' and compare it to the dc conductivity σ_0. The q dependence of $S(\omega_R')$ is illustrated in Fig. 6, where we calculated $S(\omega, q)$ from Eqs. (4), (8), (9), and (13) using the example. Included in Fig. 6 is the free-electron curve $\sigma(\omega)$. To derive an expression rigorously for $S(\omega_R', q)$ we

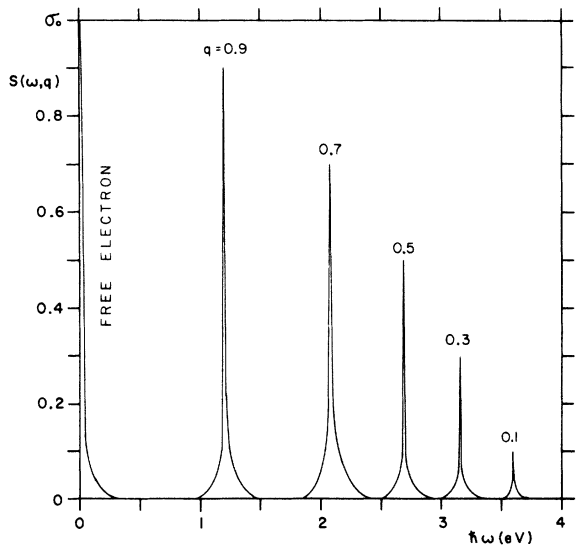

FIG. 6. Frequency dependence of optical conductivity $S(\omega, q)$ of the aggregated system at conduction resonance for various values of q, in units of the dc conductivity σ_0 of the example. Curves were calculated from exact relations (see text). Free-electron curve $\sigma(\omega)$ is also included.

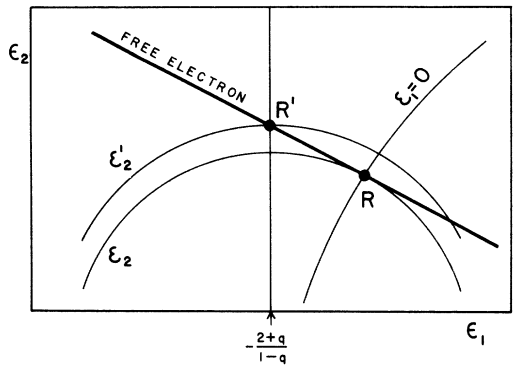

FIG. 7. An exaggerated representation of a hypothetical free-electron curve in the (ϵ_1, ϵ_2) plane, showing the relation between points R and R', to illustrate the validity of the approximation used in the text for conduction resonance.

would have to combine (4), (8), (9), and (13) but it would lead to unmanageable algebra. Instead, we use approximation.

From Fig. 3, we see that a free-electron curve lies fairly close to the ϵ_1 axis at the point $-(2+q)/(1-q)$, and is almost parallel with the ϵ_1 axis. For this reason we may consider the point at which conduction resonance occurs to be the intersection of the free-electron curve and the $\epsilon_1 = -(2+q)/(1-q)$ line, rather than the proper point at the intersection of the free-electron curve and the $\mathcal{E}=0$ contour. The details may be seen from Fig. 7, where the exact resonance point is denoted by R and the approximation by R'. The magnitude of S at resonance R is related to the value $\mathcal{E}_2$ in the figure, while the approximate maximum of S at R' is related to $\mathcal{E}_2'$ in the figure. For metals we usually have $\omega_p\tau \gg 1$, which is equivalent to the free-electron curve running close to and almost parallel with the ϵ_1 axis. From the figure it is apparent that for such a curve we have $R \approx R'$, and that our approach is reasonable.

Now we proceed with the calculation at R', leading to the expression for $S(\omega_R', q)$. The value of $\mathcal{E}_2'$ at R' from (7) is

$$\mathcal{E}_2' = 9q/[\epsilon_2'(1-q)^2], \tag{16}$$

where ϵ_2' is to be evaluated from the free-electron curve at R'. This may be done by setting $\epsilon_1 = -(2+q)/(1-q)$ in (8) and combining the result with (9), yielding

$$\epsilon_2' = [3/(1-q)][\tfrac{1}{3}A^2(1-q)-1]^{-1/2}, \tag{17}$$

where $A = \omega_p\tau$. We also get the approximate resonance frequency as

$$\omega_R' \approx [\tfrac{1}{3}\omega_p^2(1-q) - 1/\tau^2]^{1/2}. \tag{18}$$

Combining (16) and (17) gives the value of $\mathcal{E}_2$ at near resonance R' as

$$\mathcal{E}_2' = [3q/(1-q)][\tfrac{1}{3}A^2(1-q)-1]^{1/2}. \tag{19}$$

Now $S(\omega) = \mathcal{E}_2\omega/4\pi$, so $S(\omega_R', q) = \mathcal{E}_2'(q)\omega_R'/4\pi$, where $\mathcal{E}_2'(q)$ is given by (19), and ω_R' is given by (18). Note that (18) is an approximate resonance frequency, since the exact ω_R' is given by (13). Combining the relevant formulas we get

$$S(\omega_R', q) = [A^2 - 3/(1-q)]q/4\pi\tau.$$

For normal metals we have $A^2 \gg 3/(1-q)$ in the range of q values considered here (i.e., q not too close to 1), and so we get the final result for S at resonance, as

$$S(\omega_R', q) \approx \sigma_0 q, \tag{20}$$

where σ_0 is the dc conductivity of the free-electron metal.

Relation (20) tells us that the optical conductivity of an aggregated free-electron metal system at resonance is q proportion of the dc conductivity of the constituent metal. Looking back to Fig. 6, we see that this is exactly what we obtained numerically for the example. Since R is very close to R' for normal metals in the free-electron regime, the approximate relations (18) and (20) differ only a few parts in 10^4 from the exact values.

V. PLASMA RESONANCE

The effect of aggregation on the plasma frequency ω_R'' of a free-electron metal has already been con-

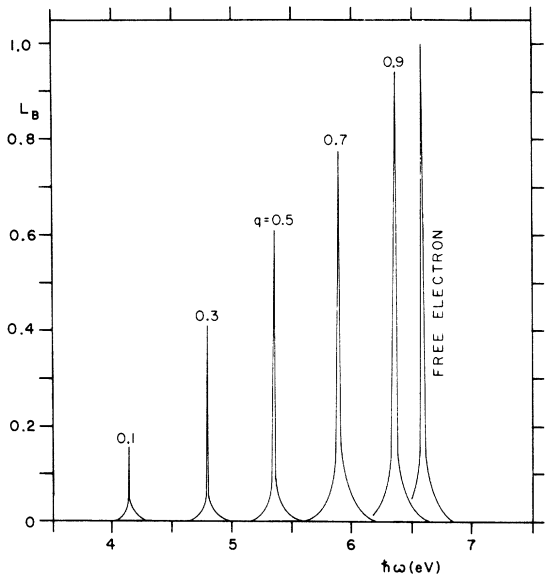

FIG. 8. Frequency dependence of the bulk electron loss function of the aggregated system at plasma resonance for various values of q, in units of the L_B for the example. The curves were calculated from exact relations (see text). Free-electron curve is also included.

sidered, and is given by (13). Here we wish to calculate the magnitude of L_B associated with the aggregated system, and compare it with that of the corresponding free-electron metal. Using the example again, we carry out the exact numerical calculation of L_B for various values of q from Eqs. (3), (4), and (8)–(10), and the plot the results in Fig. 8. Included is L_B of the free-electron metal. To derive an expression for the q-dependent maxima of L_B rigorously would be hopeless, instead, we use approximation, similar to that employed for conduction resonance.

The situation for the approximation is illustrated in Fig. 9. The exact point for plasma resonance is R, the intersection of curves $\mathcal{S}_1 = 0$, $\mathcal{S}_2$, and the free-electron curve. The approximate point is R', the intersection of the free-electron curve, and $\mathcal{S}_2'$ at $\epsilon_1 = -2(1-q)/(1+2q)$. Since a real free-electron curve lies very close to the ϵ_1 axis in the region of interest for plasma resonance, R' is very close to R and we are justified to proceed with the calculation at R'. The value $\epsilon_1 = -2(1-q)/(1+2q)$ is the intersection of the $\mathcal{S}_1 = 0$ contour with the ϵ_1 axis and may be readily obtained from (5).

The object is to express $\mathcal{S}_2'$ at this value of ϵ_1 in terms of the free-electron parameters and calculate the maximum value of L_B. From (10) we write $L_B = \mathcal{S}_2/(\mathcal{S}_1^2 + \mathcal{S}_2^2)$ and see that the maximum value for L_B given at $\mathcal{S}_1 = 0$ is $\mathcal{S}_2^{-1}$. Now we proceed with the calculation.

First, we express the approximate resonance frequency at R' by setting $\epsilon_1 = -2(1-q)/(1+2q)$ in (8). We get

$$\omega_R'' \approx [\tfrac{1}{3}\omega_p^2(1+2q) - 1/\tau^2]^{1/2} . \tag{21}$$

Note that this is an approximate relation and that the exact value of ω_R'' is given by (13). Next, we find ϵ_2 at R' by substituting ω_R'' from (21) for ω in (9). This gives

$$\epsilon_2' = [3/(1+2q)]\{\tfrac{1}{3}[A^2(1+2q) - 3]\}^{-1/2}, \tag{22}$$

where $A = \omega_p\tau$ as before. Now we take $\mathcal{S}_2$ from (4) at $\mathcal{S}_1 = 0$ and express the bulk loss function at resonance $L_B(\omega_R'', q)$. After some simplifying steps we get

$$L_B(\omega_R'', q) = \mathcal{S}_2^{-1} = \frac{9q}{\epsilon_2(1+2q)^2} + \frac{\epsilon_2(1-q)^2}{9q} . \tag{23}$$

We may neglect the second term on the right-hand side of (23) since ϵ_2 is very small, and replace ϵ_2 in (23) by ϵ_2' in (22) to get

$$L_B(\omega_R'', q) \approx Aq\,[3/(1+2q)]^{1/2} . \tag{24}$$

Now we compare the loss function of the aggregated system $L_B(\omega_R'', q)$ with that of the free-electron metal $L_B(\Omega_R'')$ directly from (24) by considering that $L_B(\Omega_R'') \approx A$. [This may be readily seen from (9) and (11) for good metals, i.e., for $A^2 \gg 1$.]

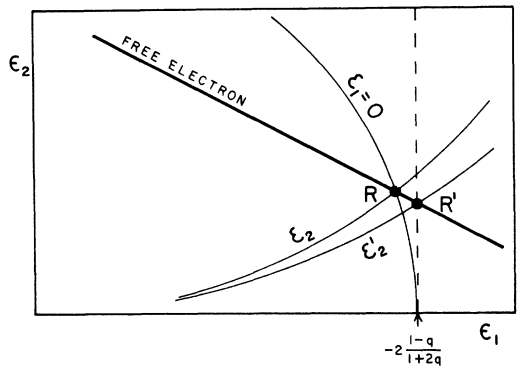

FIG. 9. An exaggerated representation of a hypothetical free-electron curve in the (ϵ_1, ϵ_2) plane showing the relation between points R and R' to help calculate plasma resonance in the text.

With this, we have the final expression for the magnitude of the q-dependent loss function at plasma resonance as

$$L_B(\omega_R'', q) \approx L_B(\Omega_R'')q\,[3/(1+2q)]^{1/2} . \tag{25}$$

A comparison of (25) and (21) with the exact numerical results, e.g., with the curves in Fig. 8, show a difference of only a few parts in 10^4, thus the relations may be considered to be very good approximations for normal metals.

VI. DISCUSSION

The main features in the optical functions of a system of free-electron metal aggregates have been derived, and are given by Eqs. (13), (18), (20), (21), and (25). The latter four are approximate relations, and apply to good metals only, while Eq. (13) gives the resonance frequencies of any aggregated free-electron system including semiconductors, etc. Deviations from free-electron processes such as interband transitions in the metal aggregates complicate the situation, and the functions can no longer be written down in a closed form. However, a graphical analysis for non-free-electron cases is still possible, and in fact is very easy, by using the MG maps such as those in Fig. 2. One may also construct the inverse transforms of the ones appearing in Fig. 2 from Eqs. (5) and (7). This would serve to interpret results obtained experimentally from materials that are known to be in aggregated form in terms of the properties of the aggregates.

It should be mentioned at this point that the frequency range in which conduction resonance is expected to occur is in the interband region for most metals, and the resulting absorption may be mistaken to be due to interband processes. Notable exceptions are some of the alkali metals discussed

elsewhere.[5] The general effect of interband processes on the conduction resonance is a marked damping, resulting in a rather broad and shallow absorption feature. This feature for real metals will be discussed in the second part.

Turning our attention back to the system of free-electron metal aggregates, it is instructive to write down one last relation. From (18) and (21), and for metals of $\omega_p \tau \gg 1$, we get

$$\omega_R'' / \omega_R' \approx [(1+2q)/(1-q)]^{1/2} . \quad (26)$$

This equation tells us that the ratio of the aggregate plasma frequency and the conduction resonance frequency is independent of the type of metal, i.e., independent of ω_p and τ in the first approximation. This may be used, in comparison with experiment, to gain information about the state of aggregation of the constituent metal. Also, if the experimental results deviate from the prediction of (26), and if the reason for this is due to $\omega_p \tau$ being not much greater than unity (which in turn may be caused by small aggregate size), then the magnitude of τ may be calculated, and the average size of the metal aggregates may be estimated.

Another important feature of (26) is that it serves to illustrate that the optical conduction resonance is not an electronic process in metals due to some weird new band structure, neither is it plasma resonance in the conventional sense. Equation (26) shows us that conduction resonance exists only in the aggregated state, that it is different from plasma resonance, and that its frequency is related to the modified plasma frequency through the aggregation parameter q only.

Next we discuss the nature of conduction resonance. The question of what is conduction resonance cannot be readily answered by the phenomenological MG theory. Instead, we offer the following model, which appears to us to be realistic. Microscopically, when light is incident on the system, one small metal aggregate finds itself in a periodic local field inside the aggregate system, and its free electrons respond to the field, sloshing back and forth within the volume of the aggregate. Since the aggregate is assumed to be much smaller than the incident wavelength, the process involves all the free electrons in the aggregate, not only the ones at the surface. This is a periodic conduction current within the aggregate causing a periodic polarization field around it—both periods being equal to that of the incident radiation. At a certain frequency the phase of conduction currents in all the aggregates become nearly equal, resulting in a strong polarization field, which enhances the local field at the aggregate. Finally, at a frequency where the real part of the dielectric constant is zero, i.e., where the local currents are exactly in phase with the driving electric field, conduction resonance occurs.

At resonance the magnitude of conductivity of each aggregate is identical with the dc conductivity and that of the whole system is q fraction of the dc conductivity of the constituent metal [see Eq. (20)]. Such high conductivity, at frequencies of a few electron volts, is not likely a normal free-electron intraband transport process at the Fermi surface. Rather, the collective oscillations at this frequency may be considered as a transverse plasma resonance.

We must be careful with transverse plasmons in metals, knowing that they cannot be supported by free electrons. In our case however, the system in which the light propagates is aggregated, and the aggregates, being separated from their neighbors, can respond to the transverse electric field.

The model advanced above is in no conflict with the results of our present analysis, neither is it physically unreal. We would expect a transverse plasmon to couple to (transverse) photons of the right frequency, and not couple to longitudinal disturbances, such as fast electrons. This is indeed what we get from the analysis, as evidenced from Figs. 4(b) and 4(c) at frequency ω_R', i.e., we have absorption of photons [Fig. 4(b)] and no electron energy loss [Fig. 4(c)]. Conversely, we would expect a longitudinal (normal) plasmon to couple to fast electrons and not to couple to photons. From the same figure we get just that at ω_R'', i.e., no photon absorption [Fig. 4(b)] and a sharp electron energy loss [Fig. 4(c)].

In spite of the attractiveness of the transverse plasmon model, we prefer to call the absorption at ω_R' conduction resonance, since this is valid in both macroscopic and microscopic views.

In the present paper, we paid no attention to surface plasmons[16] because our calculations showed no new or unusual effects due to aggregation. We want to stress, however, that conduction resonance and the resulting absorption should not be confused with surface-plasmon resonance and the resulting photon absorption. The two resonances always have different frequencies, and the absorptions caused by them differ greatly in magnitude. Moreover, surface plasmons may be excited by both photons and fast electrons, whereas conduction resonance can be excited by photons only.

In Paper II, the present results will be compared with experiment, and the effects of optical interband transitions on the conduction and plasma resonances for aggregated systems of real metals will be examined.

VII. CONCLUSIONS

The Maxwell-Garnett theory has been subjected to detailed analysis for the general case and for free-electron metals. The analysis revealed a

sharp resonance in the optical conductivity and a bulk plasma resonance for aggregated free-electron-metal systems. Formulas for the resonance frequencies and the strengths of the resonances were derived. The conduction resonance appears macroscopically to have a character of transverse plasmons, while the plasma resonance is the normal longitudinal mode. The two resonance frequencies for good metals are closely related through the aggregation parameter and are independent of the electronic parameters of the metal. The results of the present analysis lend themselves to be compared easily with experiment. The theory is being applied to real metals, and this will be the subject of the second part of this series.

ACKNOWLEDGMENTS

The authors wish to thank Professor M. Schlesinger for the helpful discussions and the Computer Center of the University of Western Ontario for their cooperation in the course of the extensive calculations.

---

*Work supported in part by the Defense Research Board of Canada, through their defense industrial research program, under DIR Project No. E 143.

[1]See, for example, M. Faraday, Phil. Trans. Roy. Soc. London A147, 145 (1857); and L. Lorenz, Wied. Ann. 11, 70 (1880).

[2]See, for example, W. T. Doyle, Phys. Rev. 111, 1067 (1958); N. Takeuchi, J. Phys. Soc. Japan 26, 872 (1969); and I. S. Radchenko, Fiz. Tverd. Tela 11, 1829 (1969) [Sov. Phys. Solid State 11, 1476 (1970)].

[3]O. S. Heavens, *Optical Properties of Thin Solid Films* (Dover, New York, 1965).

[4]E. N. Economou, Phys. Rev. 182, 539 (1969); and D. Beaglehole and O. Hundery, Phys. Rev. B 2, 309 (1970); 2, 321 (1970).

[5]J. P. Marton, Appl. Phys. Letters 18, 140 (1971).

[6]J. C. Maxwell-Garnett, Phil. Trans. Roy. Soc. London 203, 385 (1904); 205, 237 (1906).

[7]R. S. Sennett and G. D. Scott, J. Opt. Soc. Am. 40, 203 (1950).

[8]H. Mayer and B. Hietel, in *Optical Properties and Electronic Structure of Metals and Alloys*, edited by F. Abelés (Wiley, New York, 1966).

[9]G. Mie, Ann. Physik 25, 377 (1908).

[10]H. Schopper, Z. Physik 130, 565 (1951).

[11]S. Yoshida, T. Yamaguchi, and A. Kinbara, J. Opt. Soc. Am. 61, 62 (1971).

[12]D. B. McKenney and M. A. DeBell, Appl. Opt. 9, 2579 (1970).

[13]J. P. Marton, J. Appl. Phys. 40, 5383 (1969).

[14]One objection often raised against high q values is that the closest packing of spheres, hcp or fcc, gives a maximum packing density of 0.74. However, this only applies to spheres of equal diameter. Spheres with diameters ranging over one decade of values can be packed to $q > 0.9$, and as the variation of aggregate size is allowed by the MG theory, it is permissible to include high q values in the present treatment.

[15]In order to illustrate specific features of the theory, we use a hypothetical aggregated free-electron system as an example. We assume that the system satisfies the MG theory in all respects, and we chose the material constants of the constituent free-electron metal aggregates to be $\hbar\omega_p = 6.6$ eV and $\tau = 2.6 \times 10^{-14}$ sec. This is representative of normal single valence metals at room temperature. We will use this example throughout the present work and will refer to it as the "example."

[16]R. H. Ritchie, Phys. Rev. 106, 874 (1957); R. A. Ferrell, *ibid.* 111, 1214 (1958).